COHERENT RADIATION EFFECTS IN THE LCLS UNDULATOR*

S. Reiche†, UCLA, Los Angeles, CA 90095, USA
Z. Huang, SLAC, Stanford, CA 94309, USA

Abstract

For X-ray Free-Electron Lasers such as LCLS and TESLA FEL, a change in the electron energy while amplifying the FEL radiation can shift the resonance condition out of the bandwidth of the FEL. The largest sources of energy loss is the emission of incoherent undulator radiation.

Because the loss per electron depends only on the undulator parameters and the beam energy, which are fixed for a given resonant wavelength, the average energy loss can be compensated for by a fixed taper of the undulator. Coherent radiation has a strong enhancement proportional to the number of electrons in the bunch for frequencies comparable to or longer than the bunch dimension. If the emitted coherent energy becomes comparable to that of the incoherent emission, it has to be included in the taper as well. However, the coherent loss depends on the bunch charge and the applied compression scheme and a change of these parameters would require a change of the taper. This imposes a limitation on the practical operation of Free-Electron Lasers, where the taper can only be adjusted manually.

In this presentation we analyze the coherent emission of undulator radiation and transition undulator radiation for LCLS, and estimate whether the resulting energy losses are significant for the operation of LCLS.

INTRODUCTION

Recent experiments [1, 2, 3] have shown successfully the operation of free-electron lasers (FEL) in the mode of self-amplified spontaneous emission (SASE), starting from the spontaneous undulator radiation. This supports the construction of SASE FELs in the X-ray regime [4, 5]. These 4th generation light sources allows for unprecedented brightness with Ångstrom spatial and femtosecond time resolution for all branches of science [6].

For a successful operation of an X-ray FEL it is essential to keep the electron beam synchronize with the radiation field. Any externally induced loss in the electron energy will degrade the performance. However if the energy change is known it can be compensated by an adjustment in the undulator field. The dominant contribution is the emission of incoherent undulator radiation [7], which is in the case for X-ray lasers even larger than the maximum FEL signal. Other sources are undulator wakefields, which have been already presented elsewhere (e.g. [8]).

In this presentation we calculate the contribution of coherent emission of radiation, which is enhanced by the number of electron per bunch ($\approx 5 \cdot 10^9$). In particular for X-ray FELs the bandwidth of coherent emission is large because the electron bunch is strongly compressed to reduce the FEL saturation length, and thus it excites higher frequency components. In addition the particular compression scheme at LCLS [4] generates a current profile which is rather flat with spikes at the edges than Gaussian (see Fig. 1). This increases the bandwidth of the excited frequencies. The two radiation processes, which can emit coherently in an undulator, are the undulator radiation and the transition undulator radiation at the entrance and exit of the undulator.

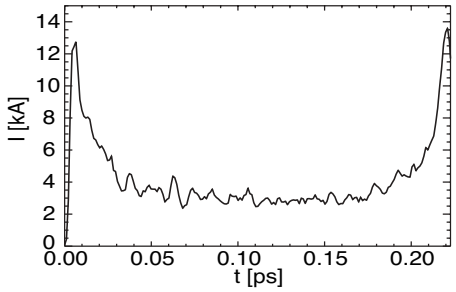

Figure 1: Current profile of the electron bunch in the LCLS undulator, calculated by start-to-end simulations.

COHERENT UNDULATOR RADIATION

Undulator radiation is the dominant radiation source and is emitted mainly in the forward direction due to the strong Doppler shift from the electron motion. The on-axis radiation can interact back on the electron beam, driving the free-electron laser mechanism. For larger emission angle with respect to the forward direction, the intensity drops quickly and the emitted wavelength is red-shifted. However beyond a threshold angle the radiation wavelength is comparable to the bunch length and the radiation adds up coherently. In the following we estimate the emitted energy due to the coherent enhancement by the particle distribution. Because we are integrating over a wide frequency range and including all directions of observation, any approximation in our calculation is excluded.

The energy emitted per solid angle and frequency interval is given by

$$\frac{d^2E}{d\omega d\Omega} = \frac{Q^2\omega^2}{16\pi^3\epsilon_0 c}|\tilde{I}(\omega)|^2 \left| \int \vec{n} \times [\vec{n} \times \vec{\beta}] e^{i\omega(t-\vec{r}\vec{n}/c)} dt \right|^2 , \quad (1)$$

with $\tilde{I}(\omega)$ the Fourier-transformed current profile, $\vec{n}$ the vector of observation, $\vec{\beta}$ the electron velocity in units of

*Work supported by the U.S. Department of Energy contract DE-AC02-76F00515

† reiche@physics.ucla.edu

the speed of light c, $\vec{r}$ the trajectory of the electron, and Q the bunch charge. For evaluation the transverse oscillation $\beta_x = K/\gamma \sin(\omega_u t)$ is in the xz-plane, where γ is the electron energy, K is the unitless undulator parameter, and $\omega_u = c\beta_0 k_u$ is the undulator wavenumber with $k_u = 2\pi/\lambda_u$ and λ_u as the undulator period. Although the longitudinal velocity β_z is modulated within a undulator period, the average velocity is given by $\beta_0 = 1-(1+K^2/2)/2\gamma^2$.

The dominant contributions in the integrations over t arise from the transverse oscillation β_x in the cross product and the transverse position r_x in the argument of the exponential function. The latter has the maximum amplitude $(\omega K/\gamma\omega_u)\sin(\theta) \ll 1$ and can be expanded in Taylor series. Both terms add up coherently as $(K/\gamma)\exp(i\omega_u t)$ with the cross product $\vec{n}\times[\vec{n}\times(\vec{e}_x + n_x(\omega/\omega_u)\vec{e}_z)]$.

The integral yield a sinc-function around the central frequency $\omega = \omega_u/(1-\beta_0\cos\theta)$, which is the resonant undulator wavelength, including the red shifting Doppler effect, when observed under an angle θ. Because the width of the sinc-function is the inverse of the number of undulator periods N_u, it selects only a narrow frequency window in the remaining integration over ω. We approximate the sinc-function by a Dirac-function $\delta(\omega_u - \omega(1-\beta_0\cos\theta))$. The integration over the frequency and the angle ϕ of the solid angle $d\Omega = \sin(\theta)d\theta d\phi$ yields

$$\frac{dE}{d\theta} = \frac{Q^2 L_u K^2 k_u^2}{32\pi\epsilon_0\gamma^2}\frac{\left(1+\left[\cos\theta - \frac{\sin^2\theta}{1-\beta_0\cos\theta}\right]^2\right)}{(1-\beta_0\cos\theta)^3} \times \sin\theta\left|\tilde{I}\left(\frac{\omega_u}{1-\beta_0\cos\theta}\right)\right|^2 . \quad (2)$$

For our calculation we consider the cases of a Gaussian and rectangular profile with the rms bunch length σ_z and form factors

$$|\tilde{I}_G(\omega)| = e^{-\omega^2\sigma_z^2} \quad \text{and} \quad |\tilde{I}_R(\omega)| = \frac{\sin^2\left(\omega\frac{\sqrt{3}\sigma_z}{c}\right)}{\omega^2\frac{3\sigma_z^2}{c^2}}.$$

Under the condition $k_u\sigma_z \ll 1$ the total emitted power is

$$E_G = \frac{Q^2 L_u K^2}{32\pi\epsilon_0\sigma_z^2\gamma^2} \quad \text{and} \quad (3)$$

$$E_R = \frac{Q^2 L_u K^2}{96\pi\epsilon_0\sigma_z^2\gamma^2}\ln\left[\frac{2\gamma^2}{1+K^2/2}\right] \quad (4)$$

for a Gaussian and rectangular current profile, respectively. For LCLS parameters ($K = 3.63$, $\gamma = 27500$ and $\sigma_z = 20$ μm) the energy losses are $E_G = 6.4$ μJ and $E_R = 40.5$ μJ, both three orders of magnitude smaller than the losses due to the incoherent undulator radiation of 17 mJ [4].

The transverse extension of the electron bunch σ_t can suppress the emission for very short bunches. Assuming a Gaussian distribution in the transverse direction the form factor of the current profile $|\tilde{I}(\omega)|^2$ has then the additional factor $\exp(-\omega^2\sigma_t^2\sin^2\theta/c^2)$. The applied correction function $S(\sigma_t/\sigma_z)$ is then

$$S(x) = 1 - x^2\sqrt{\pi}k_u\sigma_t e^{x^2k_u^2\sigma_t^2(1+x^2)} \times\left[1-\Phi\left(\frac{k_u\sigma_t}{2}(1+2x^2)\right)\right], \quad (5)$$

where Φ is the Error function. The function $S(x)$ is shown in Fig. 2. For LCLS the ratio is about 1 and the reduction in the emitted energy is negligible.

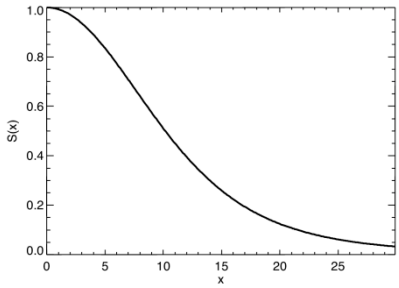

Figure 2: Suppression of the emitted energy due to the transverse size σ_t of the electron bunch. The function $S(x)$ depends on the ratio $x = \sigma_t/\sigma_z$.

COHERENT TRANSITION UNDULATOR RADIATION

Due to the transverse oscillation the average longitudinal velocity of the electron bunch is slower within the undulator than outside. The induced longitudinal acceleration of the short end pieces of the undulator, which match the straight trajectory outside of the undulator with the sinusoidal trajectory within, causes the emission of transition undulator radiation [9, 10]. The radiation footprint is similar to transition radiation [11], but there the emission is produced by the boundary condition of the electric field at the surface. A similar radiation source is edge radiation [12, 13], when an electron enters or exits the field of a bending magnet. However in transition and edge radiation the electron is modelled to come to a complete halt, while for transition undulator radiation the electron is only slowed down by $\Delta\beta = (K/2\gamma)^2$.

Low Frequency Approximation

In the low frequency model we assume that the change in the velocity is instantaneously. The emission of a single electron entering a undulator module is therefore

$$\frac{d^2E}{d\omega d\Omega} = \frac{Q^2}{16\pi^3\epsilon_0 c}\left(\frac{\beta_u\sin\theta}{1-\beta_u\cos\theta} - \frac{\beta_d\sin\theta}{1-\beta_d\cos\theta}\right)^2, \quad (6)$$

where $\beta_u = 1-(1+K^2/2)/2\gamma^2$ is the velocity within the undulator and $\beta_d = 1-1/2\gamma^2$ the velocity in the free space

outside the undulator. If the electron would be stopped completely ($\beta_u \to 0$) then the emission (Eq. 6) is identical with that of transition and edge radiation. Due to the interference of the two terms in Eq. 6 the radiation is more confined in the forward direction. Emission under large angles $\theta \gg 1/\gamma$ is suppressed by a factor γ^{-2} in comparison to transition and edge radiation.

The radiation patterns from the undulator entrance and exit interfere with each other with opposite signs and an additional phase factor $\exp(i\omega\Delta\tau)$, where $\Delta\tau = (L_m/c\beta_u)(1-\beta_u\cos(\theta))$ is the retarded time-interval when the electron enters and exits the undulator module, and L_m is the undulator module length. If the undulator consists out of N modules additional terms arising with

$$\left|\sum_{n=0}^{N-1} e^{in\omega\tau}(1-e^{i\omega\Delta\tau})\right|^2 = 4\frac{\sin^2(\omega\Delta\tau/2)\sin^2(\omega N\tau/2)}{\sin^2(\omega\tau/2)},$$

$\tau = \Delta\tau + (L_d/c\beta_d)(1-\beta_d\cos(\theta))$, and L_d the drift length, separating two adjacent undulator modules. Including also the excitation by the current profile, expressed by the form factor $\tilde{I}(\omega)$ the angular distribution per frequency interval becomes

$$\frac{d^2E}{d\omega d\Omega} = \frac{Q^2}{16\pi^3\epsilon_0 c}\left(\frac{\beta_u\sin\theta}{1-\beta_u\cos\theta}-\frac{\beta_d\sin\theta}{1-\beta_d\cos\theta}\right)^2 \times 4\frac{\sin^2(\omega\Delta\tau/2)\sin^2(\omega N\tau/2)}{\sin^2(\omega\tau/2)}|\tilde{I}(\omega)|^2. \quad (7)$$

For a typical undulator the drift between two modules corresponds to the slippage of a few resonant wavelength, which is much shorter than the bunch length. As a result the phase difference $\omega(\tau-\Delta\tau) << 2\pi$ is negligible for frequencies excited by the bunch profile. Therefore the two sine-functions $\sin(\omega\Delta\tau/2)$ and $\sin(\omega\tau/2)$ cancel each other in good approximation in Eq. 7. Effectively the undulator modules are joined together into one single long undulator module.

For very long undulator ($N\tau \gg \sigma_z/c$) the sine-function $\sin^2(\omega N\tau)$ is fast oscillating and can be approximated by its average value 1/2. In this case the integration over the frequency is decoupled from the angle of observation θ, yielding $c\sqrt{\pi/4}/\sigma_z$ and $c\sqrt{\pi^2/12}/\sigma_z$ for Gaussian and rectangular profile, respectively. The resulting emitted energy is

$$E_0 = \frac{Q^2}{2\sqrt{\pi^3}\epsilon_0\sigma_z}\left[\frac{4+K^2}{2K^2}\ln\left(1+\frac{K^2}{2}\right)-1\right] \quad (8)$$

for the Gaussian profile and is higher by the factor $\sqrt{\pi/3}\approx 1.02$ for the rectangular profile.

It is useful to point out that $N\tau$ is proportional to the slippage length of the radiation field within the undulator. The limit, discussed above, is equivalent to the condition that the bunch length is shorter than the slippage length $L_s = (\lambda/\lambda_u)z$. Otherwise the radiation is suppressed due to $\sin^2(\omega N\tau) \ll 1$ for $\omega < 2\pi c/\sigma_z$. We solve Eq. 7 numerically and express the suppression by the additional factor

$$E = E_0 \cdot F(L_s/\sigma_z) \quad . \quad (9)$$

The function F is shown in Fig.3 and is quadratic/linear for Gaussian/rectangular profile and small arguments. For LCLS the suppression is 0.01, yielding a total emitted energy of 1.3 μJ, which is comparable in its magnitude to the coherently emitted undulator radiation. It would require an undulator of about 15 km for LCLS-like parameter in order to see no suppression by the destructive interference between undulator entrance and exit.

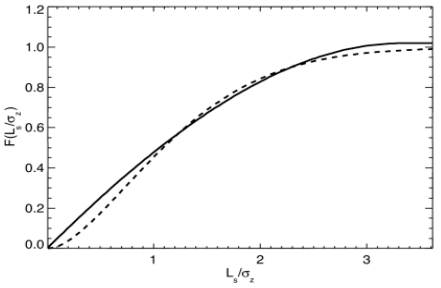

Figure 3: Function F for the suppression of the CTUR signal due to finite bunch length of a rectangular and Gaussian profile (solid and dashed line, respectively).

It seems to be counter-intuitive that the energy loss occurs over the entire undulator length, while the emission processes are spatially and temporarily localized at the entrance and exit of the undulator. But emission becomes only distinguishable in the far field zone, which lies outside the undulator. At the location of the electron the velocity field is the dominant field. In this model of undulator transition radiation the electrons are slower within the undulator and therefore the electrostatic field is less Lorentz contracted. However it is not seen be all electrons instantaneously. The change in the field is seen immediately only by the trailing electrons, while it requires some distance to catch-up with electrons ahead. This distance is the slippage length. As seen in Fig.3 the electron bunch has reached almost electrostatic equilibrium after $L_s > 3\sigma_z$ and only a negligible energy loss occurs further. At this point any retarded field information has propagated through the entire bunch.

High Frequency Limit

In the low frequency limit we assumed that the change in the velocity is instantaneously, but in reality each undulator module has a short tapering section to match the straight trajectory of the drift with the sinusoidal within. Typically the tapering section is one or two undulator periods long. Note that the characteristic frequency, which can 'probe' the explicit tapering is of the order of the res-

onant wavelength of the FEL. Thus, the low frequency approximation is valid for all current profiles, except for the micro-bunching, induced by the FEL process.

To estimate the high frequency dependence we refine our model by assuming a linear change in the velocity over the time interval δT. The acceleration is $\dot{\beta} = (\beta_u - \beta_d)/\delta T$ for entering the undulator module, yielding the profile of the electric field

$$E(\tau) = \frac{e \sin\theta}{4\pi\epsilon_0 c R} \frac{\dot{\beta}}{[(1-\beta_d \cos\theta)^2 - 2\dot{\beta}\tau\cos\theta]^{\frac{3}{2}}}, \quad (10)$$

where τ is the retarded time. The observed pulse length is $\delta\tau = (1 - \cos\theta(\beta_d + \beta_u)/2)\delta T$. The spectrum for small angle ($\theta \ll \pi/2$) is

$$\begin{aligned} \tilde{E}(\omega &= \frac{e\tan\theta}{4\pi\epsilon_0 c R}\left(\frac{e^{i\omega\delta\tau}}{1-\beta_u\cos\theta} - \frac{1}{1-\beta_d\cos\theta}\right. \\ &+ \sqrt{\pi}\varphi e^{(1-\beta_d\cos\theta)^2\varphi^2} \quad (11) \\ &\times \left.(\Phi((1-\beta_u\cos\theta)\varphi) - \Phi((1-\beta_d\cos\theta)\varphi))\right) \end{aligned}$$

with

$$\varphi = \sqrt{i\frac{\omega\delta T}{2(\beta_u - \beta_d)\cos\theta}} \quad . \quad (12)$$

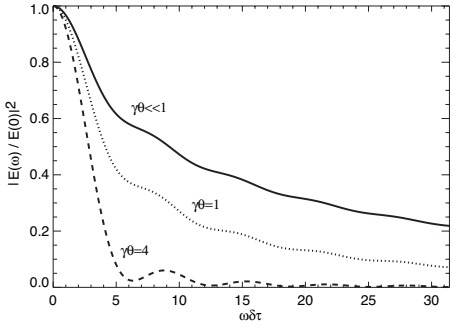

Figure 4: Power spectrum of the radiation pulse from a single electron at a single undulator entrance or exit.

Fig. 4 shows the spectra for different angle of observation. For larger value of $\theta > K/\gamma$ the pulse duration $\delta\tau$ becomes larger, resulting in a stronger suppression of emission at a given frequency. As an example a LCLS like undulator is tapered over two undulator periods. The time of observation $\delta\tau$ is about 1.7 Å$/c$ and even at the resonant wavelength at 1.5 Å the spectral power is only dropped by about 50% ($\omega\delta\tau \approx 7$) for $\theta \leq 1/\gamma$.

Because the spectrum is not suppressed significantly at the resonant wavelength, it might be considered to use CTUR as a parasitic emission signal to measure the degree of current modulation (micro bunching). With the assumption $|\tilde{I}(\omega)|^2 = |b|^2\delta(\omega - \omega_r)$ the resulting emitted energy per solid angle becomes

$$\begin{aligned} \frac{dE}{d\Omega} &= \frac{4|b|^2}{Z_0}|\tilde{E}(\omega_r,\theta)|^2 e^{-\omega_r^2\sigma_t^2\sin^2\theta/c^2} \\ &\times \frac{\sin^2(\omega_r\Delta\tau/2)\sin^2(\omega_r N\tau/2)}{\sin^2(\omega_r\tau/2)}. \quad (13) \end{aligned}$$

The radiation is strongly suppressed by two factors. First, the decoherence effect due to the finite transverse beam size confines the coherent radiation toward the forward direction $\theta \ll 1/\gamma$, where the sine-term in $\tilde{E}$ suppresses the radiation. Second, the interference of undulator entrance and exit is destructive because $\omega_r\Delta\tau$ and $\omega_r\tau$ are a integer number of π for any well tuned FEL, despite the enhancement N^2 from multiple undulator modules. However within a single undulator FEL, like the VISA FEL, the bunching occurs only within the undulator and there is no interference with the undulator entrance.

CONCLUSION

For X-ray Free-electron Laser the contributions of the coherent undulator radiation and transition undulator radiation to the overall energy loss of the electron bunch is negligible in comparison to the incoherent emission of undulator radiation. For CUR the emission is suppressed despite its enhancement by coherence because it requires the emission under an large angle so that the red shifted wavelength becomes comparable to the electron beam size. In contrast the transition undulator radiation is broadband but sees strong interference between the emission from the entrance and the exit of the undulator, which shifts the emission towards higher frequency and out of the bandwidth excited by the electron bunch. The possibility to measure the bunching factor in the FEL process is only given for long-wavelength FELs, where other methods exist to accomplish the measurement.

REFERENCES

[1] A. Tremaine *et al.*, Phys. Rev. Lett. **88** (2002) 204801

[2] S.V. Milton *et al.*, Science **292** (2001) 2037

[3] V. Ayvazyan *et al.*, Phys. Ref. Lett. **88** (2002) 104802

[4] *Linac Coherent Light Source (LCLS)*, SLAC-R-521, UC-414 (1998)

[5] TESLA-FEL 2001-05, Deutsches Elektronen Synchrotron, Hamburg, Germany (2001)

[6] C. Pellegrini and J. Stöhr, Nucl. Inst. & Meth. **A500** (2003) 33

[7] K.J. Kim, in AIP Conference Proceedings **184**, M. Month and M. Dienes, eds., (1989) 585

[8] S. Reiche and H. Schlarb, Nucl. Inst. & Meth. **A445** (2000) 155

[9] K.-J. Kim, Phys. Rev. Lett. **76** (1996) 1244

[10] B.M. Kincaid, Il Nuovo Cimento **20 D** (1998) 495

[11] V.L. Ginzburg and I.M. Frank, Zh. Eksp. Teor. Fix. **16** (1946) 15

[12] O.V. Chubar and N.V. Smolyakov, J. Optics**24** (1993) 117

[13] R.A. Bosch, Proc. of the 1999 Particle Accelerator Conference, New York (1993) 2397